

Landau Damping Simulation Models

Hua-sheng Xie (谢华生, huashengxie@gmail.com)
Institute for Fusion Theory and Simulation, Department of Physics,
Zhejiang University, Hangzhou, 310027, People's Republic of China

Oct. 4, 2013

Abstract

Several models for Landau damping simulations are provided: the simplest linear model, particle-in-cell (PIC) simulation and Vlasov continuity simulation as well as the discussions of the numerical aspects of the dispersion relation.

1 Introduction

Landau damping is one of the most interesting phenomena found in plasma physics. However, the mathematical derivation and physical understanding of it are usually headache, especially for beginners.

Here, I will tell how to use simple and short codes to study this phenomena. A shortest code to produce Landau damping accurately can be even **less than 10** lines!

2 Linear simulation model

We focus on the electrostatic 1D (ES1D) Vlasov-Poisson system (ion immobile).

The simplest method to study Landau damping is solving the following equations

$$\partial_t \delta f = -ikv \delta f + \delta E \partial_v f_0, \quad (1a)$$

$$ik \delta E = - \int \delta f dv, \quad (1b)$$

An example code can be

```
1 k=0.4; dt=0.01; nt=8000; dv=0.1; vv=-8:dv:8;
2 df0dv=-vv.*exp(-vv.^2./2)/sqrt(2*pi);
3 df=0.*vv+0.1.*exp(-(vv-2.0).^2); tt=linspace(0,nt*dt,nt+1);
4 dE=zeros(1,nt+1); dE(1)=0.01;
5 for it=1:nt
6     df=df+dt.*(-1i*k.*vv.*df+dE(it)).*df0dv;
```

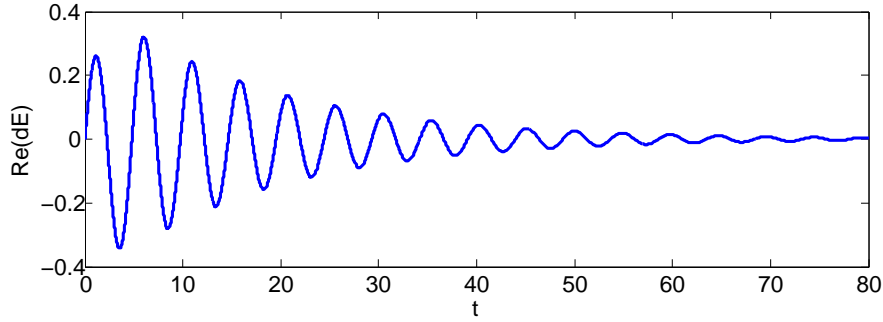


Figure 1: Linear simulation of Landau damping.

```

7     dE(i t +1)=(1 i /k)*sum(df)*dv;
8 end
9 plot(tt ,real(dE)); xlabel('t '); ylabel('Re(dE) ');

```

The simulation result is shown in Fig. 1.

Exercise 1: Solving the following fluid equations

$$\partial_t \delta n = -ik \delta u, \quad (2a)$$

$$\partial_t \delta u = -\delta E - 3ik \delta n, \quad (2b)$$

$$ik \delta E = -\delta n, \quad (2c)$$

using the above method to reproduce the Langmuir wave

$$\omega^2 = 1 + 3k^2. \quad (3)$$

3 Dispersion relation

We have seen the simplest model for Landau damping simulation in Sec. 2. How to understand the simulation results? Comparing with the analytical theory!

Dispersion relation

$$D(k, \omega) = 1 - \frac{1}{k^2} \int_C \frac{\partial f_0 / \partial v}{v - \omega/k} dv = 0, \quad (4)$$

where C is the Landau integral contour. For Maxwellian distribution $f_0 = \frac{1}{\sqrt{2\pi}} e^{-\frac{v^2}{2}}$, we will meet the well-known plasma dispersion function (PDF)

$$Z_M(\zeta) = \frac{1}{\sqrt{\pi}} \int_C \frac{e^{-z^2}}{z - \zeta} dz. \quad (5)$$

Hence, (4) is rewritten to

$$D(k, \omega) = 1 - \frac{1}{k^2} \frac{1}{2} Z'_M(\zeta) = 0. \quad (6)$$

Solving it, we obtain Table 1.

Table 1: Numerical solutions of the Landau damping dispersion relation

$k\lambda_D$	ω_r/ω_{pe}	γ_r/ω_{pe}
0.1	1.0152	-4.75613E-15
0.2	1.06398	-5.51074E-05
0.3	1.15985	-0.0126204
0.4	1.28506	-0.066128
0.5	1.41566	-0.153359
0.6	1.54571	-0.26411
0.7	1.67387	-0.392401
0.8	1.7999	-0.534552
0.9	1.92387	-0.688109
1.0	2.0459	-0.85133
1.5	2.63233	-1.77571
2	3.18914	-2.8272

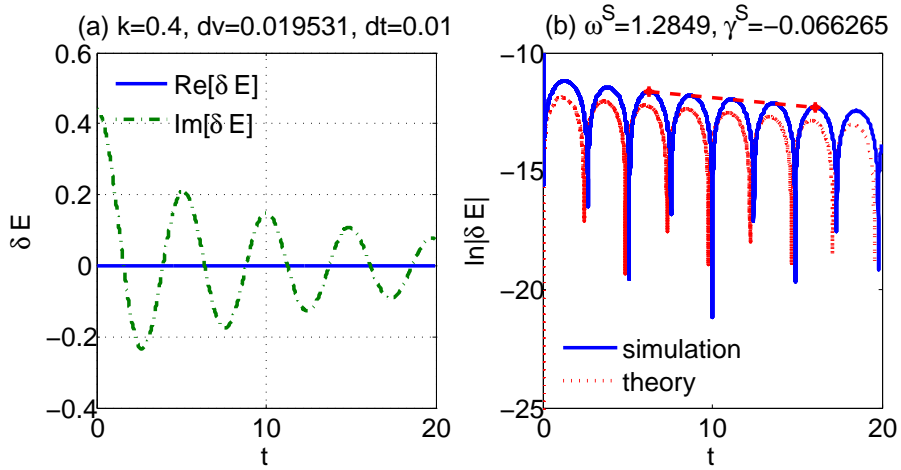


Figure 2: Linear simulation of Landau damping and compared with theory.

Adding some diagnosis lines to the code in Sec. 2, the comparison result is shown in Fig. 2. Perfect agreement is obtained: $\omega^{\text{theory}} = 1.28506 - 0.066128i$ and $\omega^{\text{simulation}} = 1.2849 - 0.06627i$

Several related topics have been omitted here, e.g., Case-van Kampen ballistic modes (eigenmode problem), non-physical recurrence effect (the Poincaré recurrence) at $T_R = 2\pi/(k\Delta v)$ [1], solving the dispersion relation with general equilibrium distribution functions (not limited to Maxwellian), advanced schemes (e.g., 4th R-K), and so on. One can refer Ref.[2] and references in for more details.

4 Particle-in-cell simulation

Normalized equations (Lagrangian approach)

$$d_t x_i = v_i, \quad (7a)$$

$$d_t v_i = -E(x_i), \quad (7b)$$

$$d_x E(x_j) = 1 - n(x_j), \quad (7c)$$

where $i = 1, 2, \dots, N_p$ is particle (marker) label and $j = 0, 1, \dots, N_g - 1$ is grid label. The particles i can be every where, whereas the field is discrete in grids $x_j = j\Delta x$, where $\Delta x = L/N_g$.

We solve the above equations in the domain $0 < x < L$ [note: $\int n(x)dx = L$], and consider periodic boundary conditions $n(0) = n(L)$ and $\langle E(x) \rangle_x = 0$. Any particle crosses the right boundary of the solution domain must reappear at the left boundary with the same velocity, and vice versa.

The initial probability distribution function [e.g., $f_0 = \frac{1}{\sqrt{2\pi}}e^{-\frac{v^2}{2}}$] is generated by N_p random numbers.

Two key steps for PIC are: 1. Field $E(x_j)$ on grids to $E(x_i)$ on particle position; 2. Particle density $n(x_i)$ to grids $n(x_j)$. Suppose that the i -th electron lies between the j -th and $(j + 1)$ -th grid-points, i.e., $x_j < x_i \leq x_{j+1}$. Usually, the below interpolation method is used

$$n_j = n_j + \frac{x_{j+1} - x_i}{x_{j+1} - x_j} \frac{1}{\Delta x}, \quad (8a)$$

$$n_{j+1} = n_{j+1} + \frac{x_i - x_j}{x_{j+1} - x_j} \frac{1}{\Delta x}. \quad (8b)$$

The above procedure is repeated from the first particle to the last particle. Similar procedure are used to mapping $E(x_j)$ to $E(x_i)$.

Code pices1d.m

```

1 close all; clear all; clc;
2 data = [0.1    1.0152    -4.75613E-15
3 0.2    1.06398    -5.51074E-05
4 0.3    1.15985    -0.0126204
5 0.4    1.28506    -0.066128
6 0.5    1.41566    -0.153359
7 0.6    1.54571    -0.26411
8 0.7    1.67387    -0.392401
9 0.8    1.7999    -0.534552
10 0.9    1.92387    -0.688109
11 1.0    2.0459    -0.85133
12 1.5    2.63233    -1.77571
13 2    3.18914    -2.8272];
14 id=7;
15 k=data(id,1);
16 wr=data(id,2); wi=data(id,3);
17
18 % parameters

```

```

19 L=2*pi/k; dt=.01; nt=1000; ntout=100; ng=32; np=50000;
20 vb=1.0; xp1=5.0e-1; vp1=0.0;
21 vt=1; % note: the normalization sqrt(2) will be found in randn()
22 wp=1; qm=-1;
23 q=wp^2/(qm*np/L); rho_back=-q*np/L; dx=L/ng;
24
25 % initial loading for the 2 Stream instability
26 xp=linspace(0,L,np)';
27 % vp=vt*randn(np,1)+(1-2*mod([1:np]',2)).*vb;
28 vp=vt*randn(np,1); % randn is {exp[-(x-mu)^2/(2*sgm^2)]}/[sgm*sqrt(2*pi)]
29
30 % Perturbation
31 vp=vp+vp1*cos(k*xp);
32 xp=xp+xp1*cos(k*xp);
33 p=1:np;p=[p p];
34
35 % Main computational cycle
36 for it=1:nt
37     % apply periodic bc on the particle positions
38     xp=xp./L+10.0; xp=L.*(xp-floor(xp));
39
40     % diagnosing
41     if(mod(it,ntout)==0)
42         plot(xp,vp,'b.','Markersize',2);
43         axis([0,L,-3*(abs(vt)+abs(vb)),3*(abs(vt)+abs(vb))]);
44         title(['Phase_space_plotting , _vp-x, _t=',num2str(it*dt)]);
45         xlabel('xp'); ylabel('vp'); pause(0.2);
46 %         print(gcf, '-dpng', ['vp-x,t=',num2str(it*dt),'.png']);
47     end
48
49     % update xp
50     xp=xp+vp*dt;
51
52     % projection p->g
53     g1=floor(xp/dx-.5)+1;g=[g1;g1+1];
54     fraz1=1-abs(xp/dx-g1+.5);
55     fraz=[fraz1;1-fraz1];
56
57     % apply bc on the projection
58     out=(g<1);g(out)=g(out)+ng;
59     out=(g>ng);g(out)=g(out)-ng;
60     mat=sparse(p,g,fraz,np,ng);
61     rho=full((q/dx)*sum(mat))'+rho_back;
62
63     % computing fields , dE/dx
64     Eg=zeros(ng,1);
65     for j=1:ng-1
66         Eg(j+1)=Eg(j)+(rho(j)+rho(j+1))*dx/2;

```

```

67     end
68     Eg(1)=Eg(ng)+rho(ng)*dx;
69     Eg=Eg-mean(Eg);
70
71     % projection q->p and update of vp
72     vp=vp+mat*qm*Eg*dt;
73
74     EEk(it)=0.5*abs(q)*sum(vp.^2); % kinetic energy
75     EEf(it)=0.5*sum(Eg.^2)*dx; % potential energy
76     t(it)=it*dt;
77 end
78
79 %%
80 h = figure('Unit','Normalized','position',...
81           [0.02 0.4 0.6 0.3], 'DefaultAxesFontSize',15);
82 subplot(121); plot(t,EEk,t,EEf,t,EEk+EEf,'r:','LineWidth',2);
83 title(['(a)  $k=$ ', num2str(k), ',  $\omega_{\text{theory}}=$ ', ...
84        num2str(wr+li*wi)], 'fontsize',15);
85 xlabel('t'); ylabel('Energy'); legend('E_k','E_e','E_{tot}',4);
86 legend('boxoff');
87
88 subplot(122);
89
90 % Find the corresponding indexes of the extreme max values
91 lndE=log(sqrt(real((EEf(1:nt))))); % EEf=E^2=[exp(gam*t)]^2=exp(2*gam*t)
92 it0=floor(nt*1/20); it1=floor(nt*17/20);
93 yy=lndE(it0:it1);
94 extrMaxIndex = find(diff(sign(diff(yy)))==-2)+1;
95 t1=t(it0+extrMaxIndex(1)); t2=t(it0+extrMaxIndex(end));
96 y1=yy(extrMaxIndex(1)); y2=yy(extrMaxIndex(end));
97 plot(t,lndE,[t1,t2],[y1,y2],'r*--','LineWidth',2);
98 omega=pi/((t2-t1)/(length(extrMaxIndex)-1));
99 gammas=(real(y2)-real(y1))/(t2-t1);
100 title(['(b)  $\omega^S=$ ', num2str(omega), ',  $\gamma^S=$ ', num2str(gammas)]);
101 axis tight;

```

Results are shown in Fig. 3. The energy conservation is very well. Real frequency and damping rate agree roughly with theory. A main drawback of PIC is the noise. Usually, very large N_p is required to reduce the influence of the noise.

5 Vlasov continuity simulation

Euler approach.

Vlasov equation

$$\partial_t f(x, v, t) = -v \partial_x f - \partial_x \phi \partial_v f, \quad (9)$$

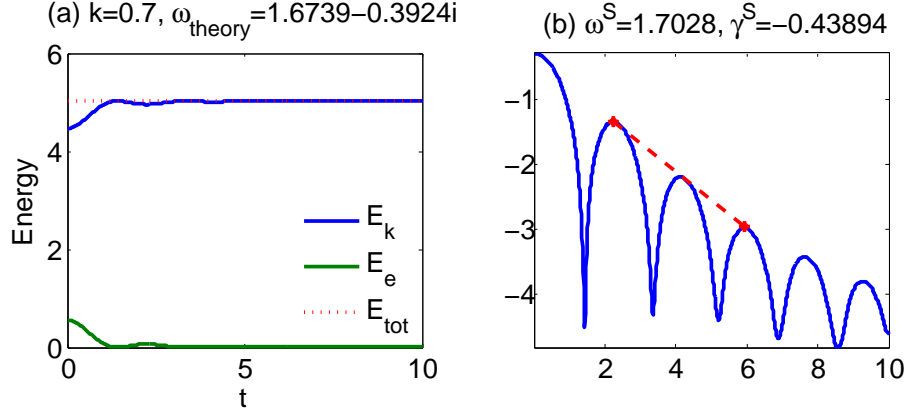


Figure 3: PIC simulation of Landau damping.

Discrete

$$\frac{f_{i,j}^{n+1} - f_{i,j}^n}{\Delta t} = -v_j \frac{f_{i+1,j}^n - f_{i-1,j}^n}{2\Delta x} - \frac{\phi_{i+1,j}^n - \phi_{i-1,j}^n}{2\Delta x} \frac{f_{i,j+1}^n - f_{i,j-1}^n}{2\Delta v}, \quad (10)$$

gives

$$f_{i,j}^{n+1} = f_{i,j}^n - v_j \frac{f_{i+1,j}^n - f_{i-1,j}^n}{2} \frac{\Delta t}{\Delta x} - \frac{\phi_{i+1,j}^n - \phi_{i-1,j}^n}{2\Delta x} \frac{f_{i,j+1}^n - f_{i,j-1}^n}{2} \frac{\Delta t}{\Delta v}. \quad (11)$$

Poisson equation

$$\partial_x^2 \phi = \int f dv - 1. \quad (12)$$

Discrete

$$\frac{\phi_{i+1} - 2\phi_i + \phi_{i-1}}{\Delta x^2} = \sum_j f_{i,j} \Delta v - 1 \equiv \rho_i, \quad (13)$$

i.e.,

$$\begin{bmatrix} -2 & 1 & 0 & \cdot & \cdot & 0 & 1 \\ 1 & -2 & 1 & \cdot & \cdot & \cdot & 0 \\ 0 & 1 & -2 & 1 & \cdot & \cdot & \cdot \\ \cdot & \cdot & \cdot & \cdot & \cdot & \cdot & \cdot \\ 1 & 0 & \cdot & \cdot & \cdot & 1 & 2 \end{bmatrix} \begin{bmatrix} \phi_1 \\ \phi_2 \\ \cdot \\ \cdot \\ \phi_N \end{bmatrix} = \begin{bmatrix} \rho_1 \\ \rho_2 \\ \cdot \\ \cdot \\ \rho_N \end{bmatrix} \Delta x^2, \quad (14)$$

where we have used the periodic boundary condition $\phi(0) = \phi(L)$, i.e., $\phi_1 = \phi_{N+1}$ and $\phi_0 = \phi_N$.

Code fkv11d.m

```

1 % Hua-sheng XIE, huashengxie@gmail.com, IFTS-ZJU, 2012-03-03 20:34
2 % fkv11d.m, 1D full-kinetic Vlasov code for unmagnetized plasma
3 % ion immobile, periodical boundary condition, phi(1)=phi(Nx+1)=0
4 close all; clear; clc;
5
6 % Landau damping data
7 data = [0.1    1.0152    -4.75613E-15
8 0.2    1.06398    -5.51074E-05
9 0.3    1.15985    -0.0126204
10 0.4    1.28506    -0.066128
11 0.5    1.41566    -0.153359

```

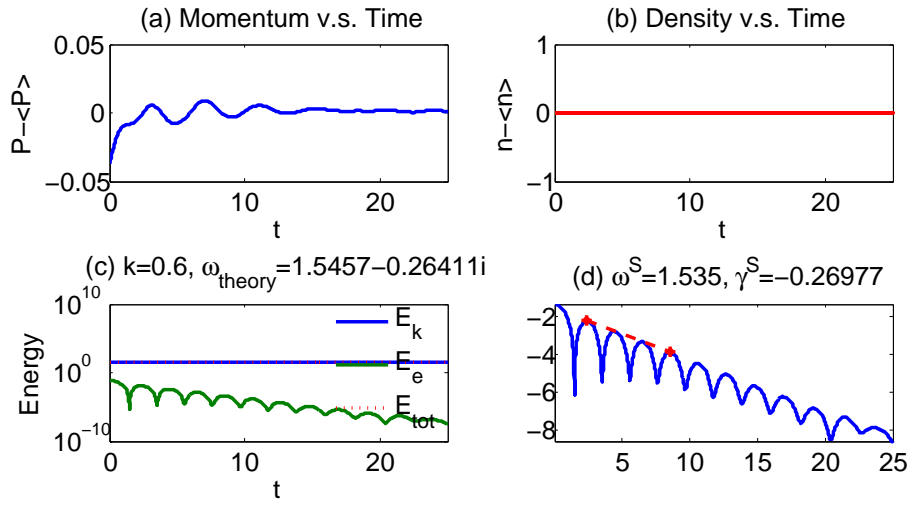


Figure 4: Vlasov continuity simulation, history plotting.

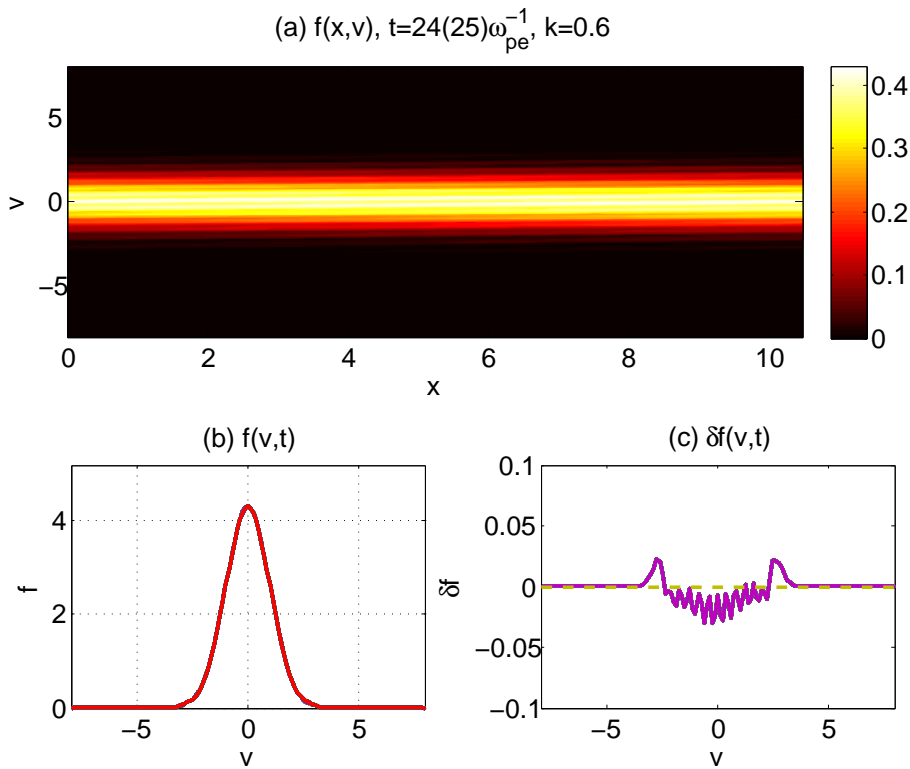


Figure 5: Vlasov continuity simulation, distribution function.

```

12 0.6 1.54571 -0.26411
13 0.7 1.67387 -0.392401
14 0.8 1.7999 -0.534552
15 0.9 1.92387 -0.688109
16 1.0 2.0459 -0.85133
17 1.5 2.63233 -1.77571
18 2 3.18914 -2.8272];
19 id=6;
20
21 k=data(id,1); wr=data(id,2); gamma=data(id,3);
22
23 nx=1*32; nv=2*64; dt=0.01; nt=5000/2; % parameters
24 L=2*pi/k; vmax=8.0; vmin=-vmax;
25 dx=L/nx; dv=(vmax-vmin)/nv;
26 fperp=0.1;
27
28 na=1.0; nb=1.0-na; vta=1.0; vtb=1.0; vda=-0.0; vdb=2.0;
29 % na=0.5; nb=1.0-na; vta=0.5; vtb=0.5; vda=-2.0; vdb=2.0;
30 % na=0.9; nb=1.0-na; vta=1.0; vtb=0.5; vda=-0.0; vdb=4.0;
31
32 vta=sqrt(2);
33
34 if(na==1.0) % for plot Landau damping theoretical results
35     tt=20;
36 else
37     tt=0;
38 end
39
40 X=0:dx:L; V=vmin:dv:vmax; [v,x]=meshgrid(V,X); % x and v grids
41 f=na*exp(-(v-vda).^2/(vta^2))/(sqrt(pi)*vta)+...
42     nb*exp(-(v-vdb).^2/(vtb^2))/(sqrt(pi)*vtb); % initial distribution
43 f=(1.0+fperp.*cos(k.*x)).*f; % initial perturbation
44
45 f(:,1)=0; f(:,nv+1)=0; % boundary in V space F must be null
46 f(nx+1,:)=f(2,:); % boundary in X space are periodic
47 f(1,:)=f(nx,:);
48
49 % f=f./((sum(sum(f))*dx*dv)/L); % re-normalized to avoid discrete errors
50 fv0=sum(f,1)*dx; maxfv0=max(fv0);
51
52 rho_back=1.0; % /L
53
54 dtodx=dt/dx; dtodv=dt/dv; dx2=dx*dx;
55
56 un=ones(nx,1);
57 poisson=spdiags([un -2*un un],[-1 0 1],nx,nx);
58 poisson(1,nx)=1;poisson(nx,1)=1; % phi(nx+1)=phi(1), phi(0)=phi(nx)
59

```

```

60 figure('position',[100 100 800 600]);
61 set(gcf,'DefaultAxesFontSize',15);
62 set(gca,'nextplot','replacechildren');
63 ifig=1;
64
65 for it=1:nt
66
67     rho=sum(f,2)*dv-rho_back; % computing density
68
69     phi=poisson\rho(1:nx)*dx2; % computing fields
70     phi=[phi;phi(1)]; % ./rho_back
71     Ex=( [phi(nx+1); phi(1:nx)] - [phi(2:nx+1);phi(1)] )/(2*dx);
72     Ex(nx+1)=Ex(1);
73
74     for j=2:nv % computing PDF
75         f(1,j)=f(1,j)-V(j)*(f(2,j)-f(nx,j))/2*dtodx+...
76             Ex(1)*(f(1,j+1)-f(1,j-1))/2*dtodv;
77         for i=2:nx
78             f(i,j)=f(i,j)-V(j)*(f(i+1,j)-f(i-1,j))/2*dtodx+...
79                 Ex(i)*(f(i,j+1)-f(i,j-1))/2*dtodv;
80         end
81     end
82
83     f(:,1)=0; f(:,nv+1)=0; % boundary in V space F must be null
84     f(nx+1,:)=f(1,:); % boundary in X space are periodic
85
86     den=sum(f,2)*dv; % density
87     P=sum(v.*f,2)*dv; % momentum
88     Ek=sum((v.^2).*f,2)*dv; % kinetic energy
89     t(it)=it*dt;
90     Den=sum(den); % density history
91     PP(it)=sum(P); % momentum history
92     EEk(it)=sum(Ek); % kinetic energy history
93     EEf(it)=0.5*sum(Ex.*Ex)*dx; % field energy history
94
95     if(mod(it,floor(nt/200)*10)==0) % diagnose
96         pause(0.001);
97
98         subplot(2,2,1:2);
99         colormap(hot);
100        [C,h]=contourf(x,v,f,50); colorbar;
101        set(h,'Color','none');
102        title(['(a) f(x,v), t=', num2str(it*dt), '( ', num2str(nt*dt), '...
103            ')\omega_{pe}^{-1}, k=', num2str(k)], 'fontsize',15);
104        xlabel('x'); ylabel('v');
105
106        subplot(2,2,3);
107        fv=sum(f,1)*dx;

```

```

108     plot(v, fv0, '--', v, fv, '-', 'LineWidth', 2); grid on;
109     title('(b) f(v, t)'); xlabel('v'); ylabel('f');
110     ylim([0, 1.2*maxfv0]); xlim([vmin, vmax]);
111
112     subplot(2, 2, 4);
113     plot(v, fv-fv0, '-', [vmin, vmax], [0, 0], '--', 'LineWidth', 2);
114     title('(c) \delta f(v, t)'); xlabel('v'); ylabel('\delta f');
115     xlim([vmin, vmax]);
116     ylim([-1*fperp*maxfv0, 1*fperp*maxfv0]);
117     ylim([-1*fperp, 1*fperp]);
118
119     Fig(iframe)=getframe(gcf, [0, 0, 800, 600]);
120     iframe=iframe+1;
121     end
122 end
123 print(gcf, '-dpng', 'plot_fxv.png');
124 movie(Fig);
125 writemovie('movie_fxv.gif', Fig, 0.1);
126 % close all;
127
128 %%
129 h = figure;
130 set(gcf, 'DefaultAxesFontSize', 15);
131 subplot(221); plot(t, PP-mean(PP), 'LineWidth', 2); xlim([0, max(t)]);
132 title('(a) Momentum v.s. Time', 'fontsize', 15); xlabel('t'); ylabel('P-<P>');
133 subplot(222); plot(t, Den-mean(Den), 'r', 'LineWidth', 2); xlim([0, max(t)]);
134 title('(b) Density v.s. Time', 'fontsize', 15); xlabel('t'); ylabel('n-<n>');
135 subplot(223);
136 semilogy(t, EEk, t, EEf, t, EEk+EEf, ':', 'LineWidth', 2);
137 title(['(c) k=', num2str(k), ', \omega_{theory}=', ...
138       num2str(wr+1i*gamma)], 'fontsize', 15);
139 xlabel('t'); ylabel('Energy'); legend('E_k', 'E_e', 'E_{tot}', 4);
140 legend('boxoff'); xlim([0, max(t)]);
141
142 subplot(224);
143 % Find the corresponding indexes of the extreme max values
144 lndE=log(sqrt(real((EEf(1:nt))))); % EEf=E^2=[exp(gam*t)]^2=exp(2*gam*t)
145 it0=floor(nt*1/20); it1=floor(nt*7/20);
146 yy=lndE(it0:it1);
147 extrMaxIndex = find(diff(sign(diff(yy)))==-2)+1;
148 t1=t(it0+extrMaxIndex(1)); t2=t(it0+extrMaxIndex(end));
149 y1=yy(extrMaxIndex(1)); y2=yy(extrMaxIndex(end));
150 plot(t, lndE, [t1, t2], [y1, y2], 'r*--', 'LineWidth', 2);
151 omega=pi/((t2-t1)/(length(extrMaxIndex)-1));
152 gammas=(real(y2)-real(y1))/(t2-t1);
153 title(['(d) \omega^S=', num2str(omega), ', \gamma^S=', num2str(gammas)]);
154 axis tight;
155

```

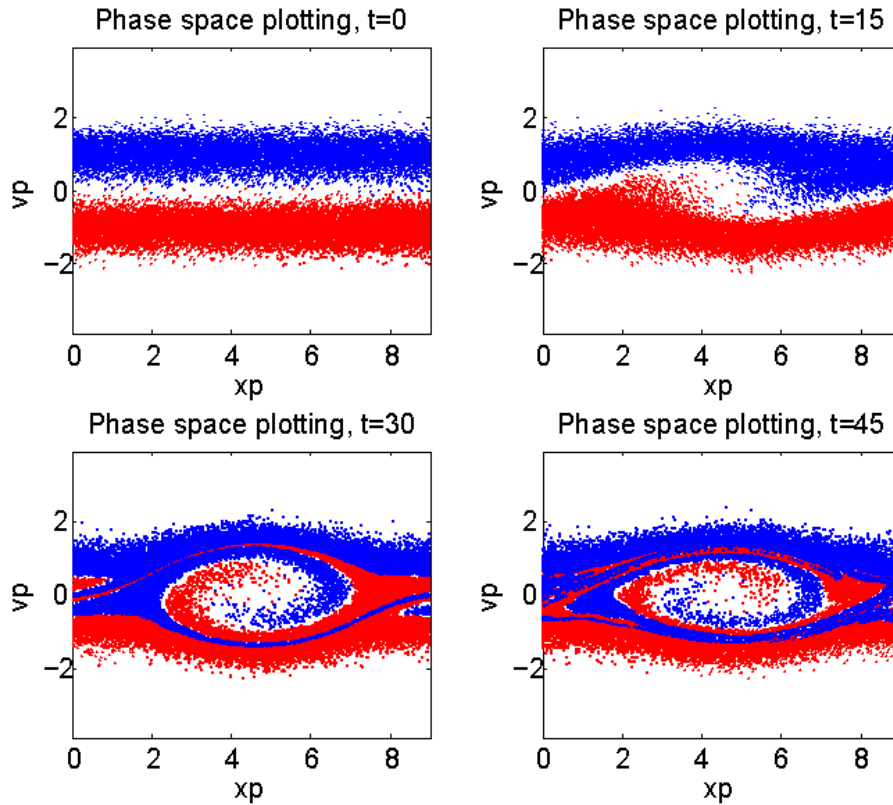


Figure 6: PIC simulation of the two-stream instability, phase space plotting.

```

156 print(h, '-dpng', 'plot_diag.png');
157 % close all;

```

writegif.m can be found using Google.

The results are shown in Fig. 4 and Fig. 5. Real frequency and damping rate are consistent with theory.

6 Nonlinear simulations

The PIC and Vlasov codes provided in the above sections can be easily modified to study the linear and nonlinear physics of the beam-plasma or two-stream instabilities.

A PIC simulation of two-stream instability is shown in Fig. 6 and Fig. 7. The linear growth and nonlinear saturation are very clear.

Exercise 2: Solving the kinetic or fluid dispersion relations for beam-plasma or two-stream plasma and comparing the results with linear and nonlinear simulations using the above models.

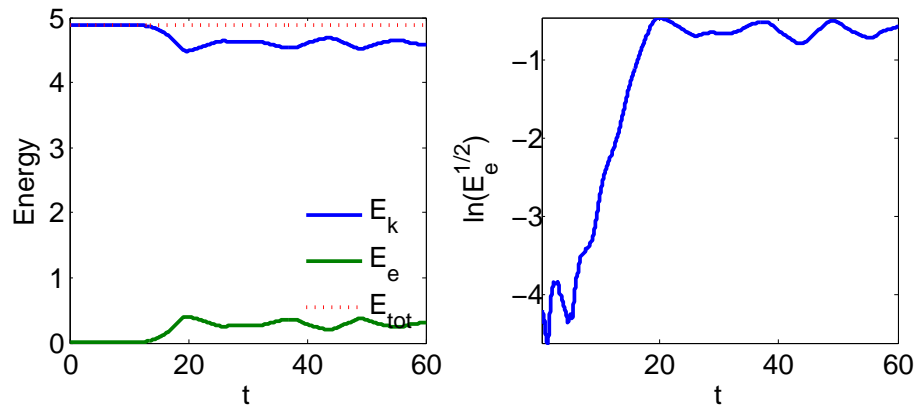


Figure 7: PIC simulation of the two-stream instability, history plotting.

References

- [1] C. Z. Cheng and G. Knorr, The integration of the vlasov equation in configuration space, *Journal of Computational Physics*, 22, 330 - 351, 1976.
- [2] H. S. Xie, Generalized Plasma Dispersion Function: One-Solve-All Treatment, Visualizations, and Application to Landau Damping, *Phys. Plasmas*, 20, 092125, 2013. Also, <http://arxiv.org/abs/1305.6476>. With codes.